RMetS
Royal Meteorological Society

The link between cut-off lows and Rossby wave breaking in the Southern Hemisphere

Thando Ndarana[a,b]*and Darryn W. Waugh[b]
[a]*South African Weather Service, Pretoria, South Africa*
[b]*Department of Earth and Planetary Sciences, Johns Hopkins University, USA*
*Correspondence to: Thando Ndarana, South African Weather Service, Private Bag x 097, Pretoria 0001, South Africa.
E-mail: thando.ndarana@weathersa.co.za

The climatological link between cut-off low (COL) pressure systems that occur from 20 to 50 S and Rossby wave breaking (RWB) in the Southern Hemisphere (SH) is examined for 1979–2008. It is shown that COLs are associated with either RWB events (89%) or with potential vorticity (PV) intrusions where there is north–south advection of high-PV air (11%). In the vast majority of COLs, the RWB events occur upstream, on or before the day of the COL formation. The evolution of the PV, geopotential heights, static stability, absolute vorticity and temperature advection fields during the COLs are consistent with the formation of high-PV anomalies that induce cyclonic circulations as predicted by theory. RWB plays a key role in producing the split flow associated with COLs in the SH, which in turn produces absolute vorticity anomalies by shear-curvature vorticity conversion, and creates static stability anomalies. The COLs associated with RWB at 330 K are deeper and more persistent than those associated with 350 K RWB and surface processes differ depending on the isentropic surface on which the associated RWB occurs. The seasonality of the RWB and COLs are similar, and is linked to the seasonal march of the westerly jets. Copyright c 2010 Royal Meteorological Society

Key Words: potential vorticity anomaly; potential vorticity intrusion; jet stream

Received 23 October 2009; Revised 15 March 2010; Accepted 24 March 2010; Published online in Wiley InterScience 4 May 2010

Citation: Ndarana T, Waugh DW. 2010. The link between cut-off lows and Rossby wave breaking in the Southern Hemisphere. *Q. J. R. Meteorol. Soc.* **136**: 869–885. DOI:10.1002/qj.627

1. Introduction

Cut-off low (COL) pressure systems are closed, cold-cored low pressure systems that have been detached from the main westerlies aloft (Palmén and Newton, 1969). The systems are baroclinic and their development is associated with cold fronts and therefore cold air advection at the surface (Matsumoto *et al.*, 1982; Taljaard, 1985). COLs are capable of producing heavy rainfall and floods. For example, over South Africa 20% of all floods result from these systems (Taljaard, 1985; Singleton and Reason, 2007). COLs also play a role in the stratosphere–troposphere exchange (Price and Vaughan, 1993) and can be responsible for changes in tropospheric ozone concentrations (e.g. Ancellet *et al.*, 1994; Barsby and Diab, 1995; Oltmans *et al.*, 1996). From the above, it follows then that improved understanding of COL systems is highly desirable for weather forecasting and understanding the composition of the troposphere.

Several case-studies have considered COLs from a potential vorticity (PV) perspective (e.g. Bell and Keyser, 1993; van Delden and Neggers, 2003). Such studies have shown that COL pressure systems are associated with high-PV anomalies caused by the isentropic and equatorward advection of stratospheric air into the troposphere as suggested by Hoskins *et al.* (1985). This advection could be quasi-horizontal (Hoskins *et al.*, 1985) or could also have a strong downward vertical component (cf. Thorncroft *et al.*, 1993, their Figure 1). Inside the low, air of stratospheric

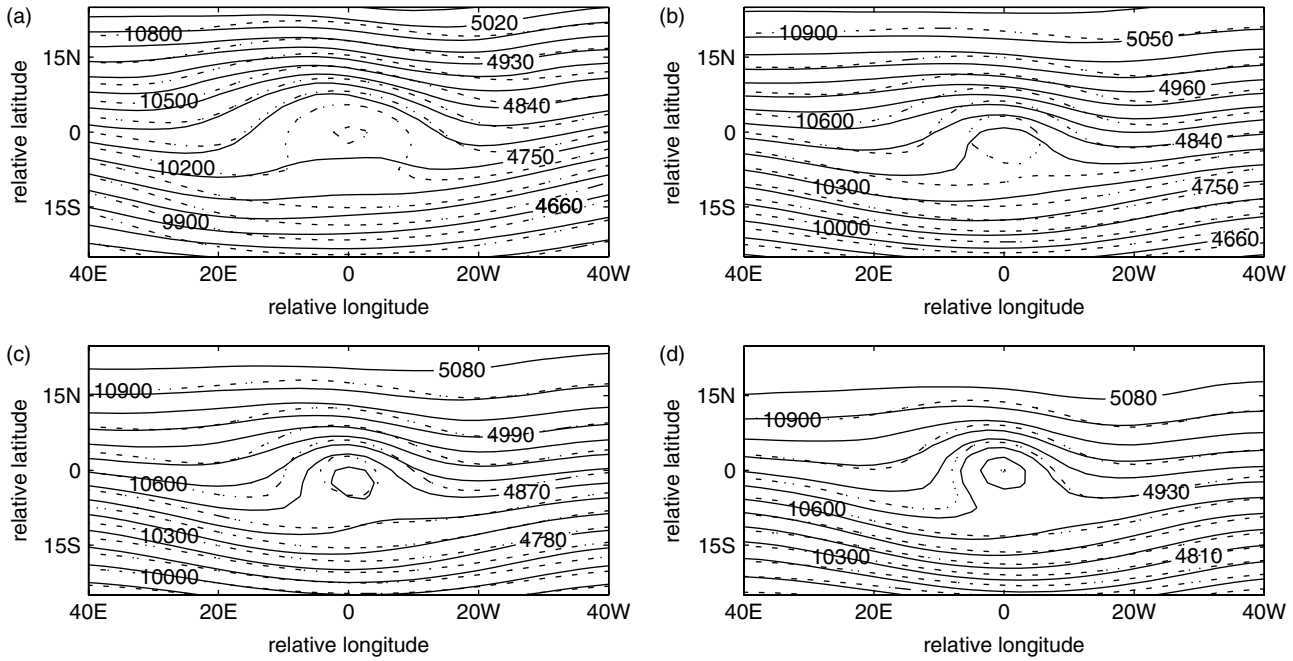

Figure 1. Composites mean fields of geopotential height at 250 hPa (dashed contours with interval 100 m) and 250–500 hPa thickness (solid contours with interval 30 m). The panels correspond to (a) one, (b) four, (c) five and (d) eight immediate neighbours of the COL centre being warmer than the centre.

origin is transported across the isentropes in the vertical direction (Price and Vaughan, 1993).

The high-PV anomalies associated with the COLs are likely to be residues of the Rossby wave breaking (RWB) process. RWB is defined as the rapid and irreversible deformation of PV material contours (McIntyre and Palmer, 1983) such that the meridional PV gradient reverses (Baldwin and Holton, 1988; Postel and Hitchman, 1999; Hitchman and Huesmann, 2007). During the late stages of certain types of the RWB process, blobs of high-PV air form (e.g. Appenzeller and Davies, 1992; Thorncroft *et al.*, 1993; Appenzeller *et al.*, 1996).

Cases of COLs viewed from an isobaric surface that occur simultenously with RWB events have been observed (e.g. Langford *et al.*, 1996; Baray *et al.*, 2005). Furthermore, Price and Vaughan (1993) noted that tropopause folds, which are examples of RWB, likely accompany the occurrence of COLs. This suggests that there might be a link between COLs and RWB. However, whether or not this link is climatological is, to the best of our knowledge, still an open question. Therefore the primary aim of this paper is to conduct a quantitative study to show that COLs can be linked to RWB in the Southern Hemisphere (SH).

The general behaviour of COLs has been studied by forming climatologies in both hemispheres. In the Northern Hemisphere (NH), Kentarchos and Davies (1998) found, using a subjective approach, that COLs tend to occur more often in summer than in winter at 200 hPa. This was confirmed by Nieto *et al.* (2005) in an objective hemispheric-wide study using a much longer dataset. Both studies suggest that the seasonal variability of COLs is related to that of jet streams; that is, COLs tend to form when the jets are weaker. Furthermore, Kentarchos and Davies (1998) also found that subtropical COLs have smaller temporal and spatial scales than their midlatitude counterparts. Climatologies of COLs from a PV perspective have also been formed for the NH (e.g. Wernli and Sprenger, 2007; Nieto *et al.*, 2008). The geographical distribution of high isentropic PV anomalies was found to be consistent with that of COLs viewed from isobaric surfaces.

In the SH, regional studies have been conducted at various levels. Taljaard (1985) and Singleton and Reason (2007) considered 300 hPa COLs over the South African region and immediate surrounding oceans. They showed that COLs are most frequent during the autumn and occur the least during the summer. Over South America, Campetella and Possia (2007) found that at 250 hPa they are more frequent during the equinox seasons and are minimal during the other seasons. Also Qi *et al.* (1999), using geopotential height charts at 500 hPa, found that over the Australian region these systems occur the most during the colder parts of the year. From the above studies, the variability of COLs is clearly influenced by local meteorological and orographical processes.

Fuenzalida *et al.* (2005) conducted the first hemispheric-wide study in the SH at 500 hPa, using a combination of objective and subject methodology. In their study they also addressed the regional interseasonal variability of these systems. More recently, Reboita *et al.* (2009) extended the work of Nieto *et al.* (2005) to the SH and produced a hemispheric climatology of COLs at 200 hPa. These two SH climatologies show that there are significant differences in the interseasonal variability of COLs between levels: Fuenzalida *et al.* (2005) found higher frequencies during winter, in contrast to the summer maximum found by Reboita *et al.* (2009). Therefore, the secondary aim of this study is to understand the variability of COLs at different levels in the SH.

The outline of the paper is as follows. In section 2, data and methods of identifying COLs and RWB events are outlined. The climatology of COLs in the SH at 250 hPa is presented in section 3. In section 4 the link between COLs and RWB is established and the influence of RWB on COL formation and variability are examined. COLs that are not associated with

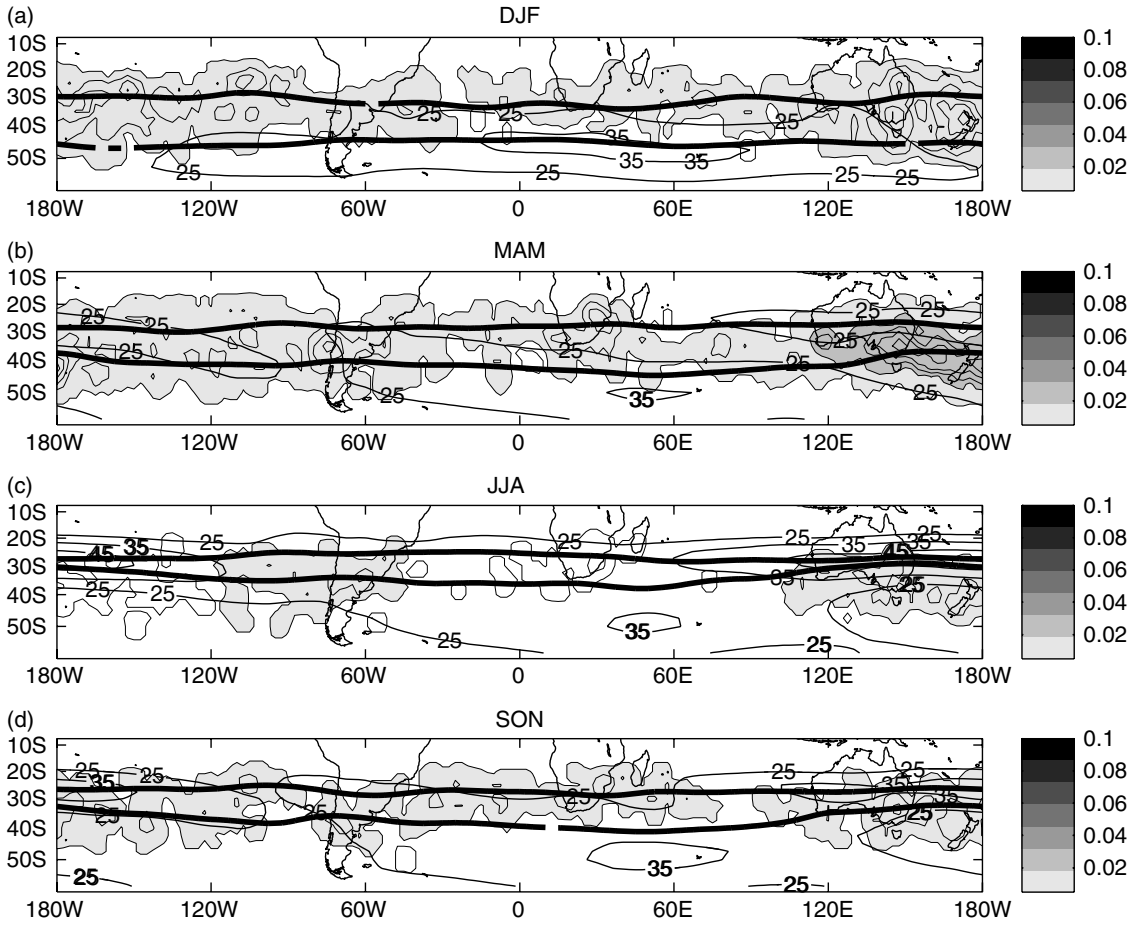

Figure 2. Geographical distribution of COLs at 250 hPa per season for the period 1979–2008. The frequencies at each grid point are smoothed using a 5 5 running mean, and shaded contours are at intervals of 0.02 y ^{1}. The bold solid contours represent the PV = –2 PVU contours on the 350 K (northern) and 330 K (southern) isentropic surfaces. The thin solid contours are the zonal mean winds at 10 m s ^{1} intervals.

RWB are then analysed in section 5. Concluding remarks are in section 6.

2. Data and methods

2.1. Data

We use the National Centers for Environmental Prediction/National Center for Atmospheric Research (NCEP/NCAR) reanalysis fields (Kalnay *et al.*, 1996) to identify COLs and RWB events from 1979 to 2008. Both processes have been established to have durations longer than one day (e.g. Peters and Waugh 1996; Fuenzalida *et al.*, 2005; Nieto *et al.*, 2005; Reboita *et al.*, 2009). Thus for our purposes it suffices to use daily averaged reanalysis data (from four times each day). These data are on a grid with a horizontal resolution of 2.5 2.5 on all tropospheric standard levels.

PV is calculated on isobaric surfaces from daily velocity and temperature fields (cf. Hoskins *et al.*, 1985, Eq. 13). The spatial derivatives of the velocity fields are calculated using second-order centred differences and the stability expression used is similar to that in Trenberth (1991). The resulting isobaric PV fields are then linearly interpolated to 310, 330 and 350 K isentropic surfaces, as in Edouard *et al.* (1997).

The quality of NCEP/NCAR reanalysis in the SH is questionable prior to 1979. Unlike the NH, the SH was poorly observed during this era because it is mostly covered by oceans (Tennant, 2004). Improvements to this state of affairs occurred in 1979 with the introduction of the Television Infrared Observation Satellite (TIROS) Operational Vertical Sounder (TOVS) (Kistler *et al.*, 2001). Consequently, this study will be restricted to the period 1979 onwards.

2.2. COL diagnostics

The methodology used to define COLs is very similar to that of Nieto *et al.* (2005) and Reboita *et al.* (2009), with a more explicit imposition of the cold-core condition similar to that in Fuenzalida *et al.* (2005). The algorithm is a multiple step process, and has been applied to identify COLs on different pressure surfaces.

A visual inspection of daily zonal profiles of isentropic surfaces, geopotential heights and the dynamical tropopause (represented by the PV = –2 PVU surface, where 1 PVU = 10 ^{6}m^{2}s ^{1}K kg ^{1}) indicates that meteorological processes that occur on the 250 hPa surface are placed in close proximity to both the subtropical and midlatitudinal dynamical tropopause positions. The 200 hPa (300 hPa) surface is too high (low) to be associated with PV/isentropic processes occurring on the 330 K (350 K) dynamical tropopause. As a consequence, for purposes of linking COLs to RWB on the dynamical tropopause, we will focus primarily on 250 hPa COLs, but briefly consider 500 hPa COLs for purposes of the second question that was mentioned in the Introduction.

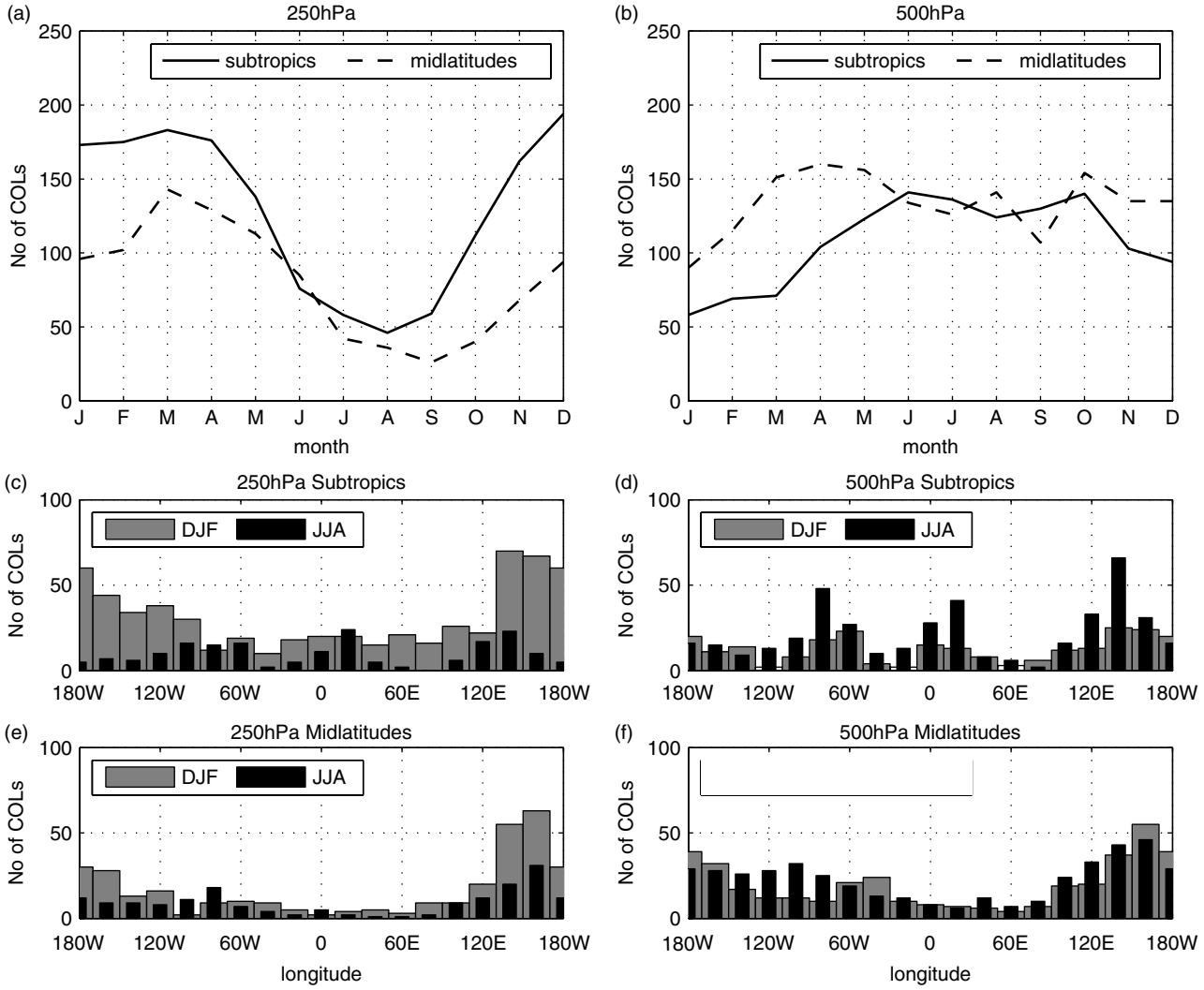

Figure 3. Climatology of COLs identified during the period 1979–2008. (a) Frequency of COLs on the 250 hPa surface as a function of month in the Subtropics (north of 35 S, dashed) and in midlatitudes (south of 35 S, solid). (b) is as (a), but for the 500 hPa isobaric level. (c) Frequency of COLs as a function of longitude in the Subtropics on the 250 hPa surfacein summer (DJF) and winter (JJA). (d) is as (c), but for the Subtropics on the 500 hPa isobaric level. (e, f) are as (c, d), but for the midlatitudes.

The first step involves identifying minima on the 250 hPa (or 500 hPa) geopotential height fields on each day during the study period. A grid point is considered a potential COL point if its geopotential height value is lower than those of at least six of the eight immediate surrounding points by at least 10 gpm (Nieto *et al.*, 2005; Reboita *et al.*, 2009). Furthermore, the 250 hPa zonal wind is required to change direction at one or two of the grid points immediately south of all those satisfying the geopotential height minimum condition. As an additional measure, these grid points must be surrounded by a closed isohypse. This eliminates all those points that are associated with troughs that do not have a closed circulation.

The second step imposes a cold-core condition on all potential COLs systems identified in the manner just described using the thickness fields of the 250–500 hPa layer (500–850 hPa for COLs at 500 hPa). Thickness fields are preferable to the temperature fields because they are more representative of the thermal properties of the layer, as prescribed by the hypsometric relation. In this step, each potential COL point is required to be colder than its surroundings. Sensitivity tests were performed by varying the number of points that are warmer than the COL point from one to eight and the cold pool of air forms for five or more warmer neighbouring grid points, as shown by composite mean thickness and geopotential fields (Figure 1). Details of how composites are formed will follow in section 2.4.

This step differs from the corresponding step in Nieto *et al.* (2005). The use of the equivalent thickness leads to a gross underestimation of the number of COLs in the SH. The cold-core condition used by Taljaard (1985), Fuenzalida *et al.* (2005) and Campetella and Possia (2007) is consequently the preferred method in this study. As noted in the Introduction, these weather systems have been well established to have such a cold core (e.g. Matsumoto *et al.*, 1982; Hoskins *et al.*, 1985). The choice of the 250–500 hPa thickness layer is motivated by the funnel structure of the vertical cross-section of COL systems (e.g. Palmén and Newton, 1969; Hoskins *et al.*, 1985). The lower tip of the funnel is at about 500 hPa.

Because of the choice made in the second step, the implementation of the thermal front parameter condition as in Nieto *et al.* (2005), and even the modified version (Reboita *et al.*, 2009), also underestimates COLs in the SH. This suggests that this parameter is best used together

with the equivalent thickness rather than with the explicit cold-core condition as used in this study.

After the completion of the above steps, we found that in some cases several selected grid points belonged to the same COL system on the same day. To eliminate duplications, the grid point with the lowest geopotential height within 10 10 regions for a given day was selected.

While a percentage of these systems is quasi-stationary, COLs in the SH can attain speeds of about 2200 km d ^{1}, and in some cases more (Fuenzalida *et al.*, 2005; Reboita *et al.*, 2009), toward the east and may also retrogress. They are also capable of reaching meridional speeds of about 800 km d ^{1} (Fuenzalida *et al.*, 2005). On this basis, each COL that is within 10 latitude (with 2.5 275 km) and 20 longitude from a COL that occurred the day before is considered a duplicate count and is removed from the database. Finally, we consider only those systems that occur within the 20–50 S latitude band, which excludes tropical and polar lows. The resulting dataset contains dates of the inception of the systems and their positions.

The above procedure has been applied to daily data from January 1979 to December 2008 to form a 30-year climatology of COLs at 250 hPa and 500 hPa.

2.3. *RWB diagnostics*

We focus on RWB events that occur on PV = –1.5 to –2.5 PVU contours on the 310, 330 and 350 K isentropic surfaces. These PV contours on these surfaces represent the dynamical tropopause in the high latitudes, midlatitudes and Subtropics, respectively.

To identify the RWB events, we employ an objective algorithm that uses the geometry of the overturning contours which represents the RWB process (e.g. Esler and Haynes, 1999; Postel and Hitchman, 1999). This is also a multi-step process.

First, subsynoptic-scale features are filtered out from the PV by spectral truncation, leaving only the zonal mean and the first ten wavenumbers. Then on each day and for each of the three PV contours, potential RWB events are identified when a meridional line intersects a PV contour at two or more latitudes (cf. Figure 5a in Esler and Haynes, 1999). When these intersections are found, their times, longitudes and latitudes are recorded. If grid points that are identified in this manner have equal or consecutive longitudes then they belong to the same RWB event.

This method inherently captures closed contours that represent secluded stratospheric and tropospheric air blobs (closed high- and low-PV anomalies). To exclude such isolated features from the database, we apply it only to contours that have more than 144 grid points; this ensures that each contour that we consider is as long as a latitude circle or longer. All the grid points that satisfy the above condition are located on the portion of the contour that represents the fold of the contour.

Some of these folds are small scale; to remove these we require that potential RWB events comprise more than 20 grid points. The algorithm also captures some parts of the contours that extend equatorward/poleward without overturning. To combat this problem, we further require the grid points in the interior of the folds to have a reversed meridional PV gradient (Baldwin and Holton, 1988; Postel and Hitchman, 1999; Hitchman and Huesmann, 2007) and then store the westernmost point that satisfies this condition.

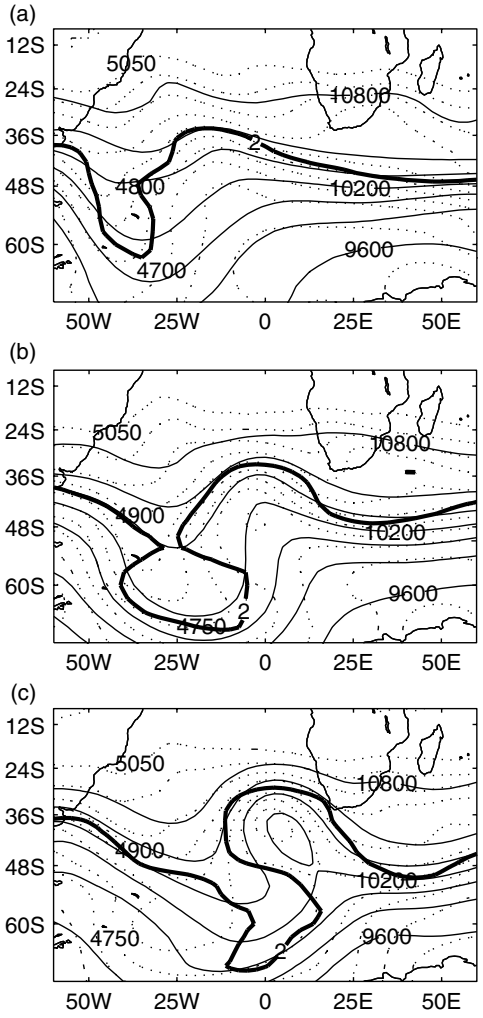

Figure 4. Evolution of 250 hPa geopotential height (thin solid contours with interval 200 gpm), 250–500 hPa thickness (dashed contours with interval 50 gpm) and PV = –2 PVU contour (bold solid) on the 330 K surface at 0000 UTC on (a) 15, (b) 16 and (c) 17 April 1985.

In some cases, the same RWB event occurs on two or all three contours simultaneously. In such situations, only one of the points is recorded. Finally, to ensure that each RWB event is accounted for only once, the algorithm keeps only the count that is associated with the onset of the event. The resulting database contains the dates, longitudes, latitudes and the values of the PV contour for the onset of RWB events.

2.4. *Composite analysis*

Much of the discussion in this paper employs composite analysis. The methodology used is similar to that of Waugh and Funatsu (2003). In this analysis we calculate averages of different fields over all COL events. This is done for the day of the COL (day 0), as well as for each day between 5 d before (day –5) and 5 d after (day +5) the formation of the COL, but we only show composite calculations for day –3 to day +2. When forming the averages, the fields are shifted in longitude and latitude so that the centres of the COL coincide. The maps of composite-average fields shown in section 4.2 then use longitude and latitude relative to the COL centre as the horizontal coordinates.

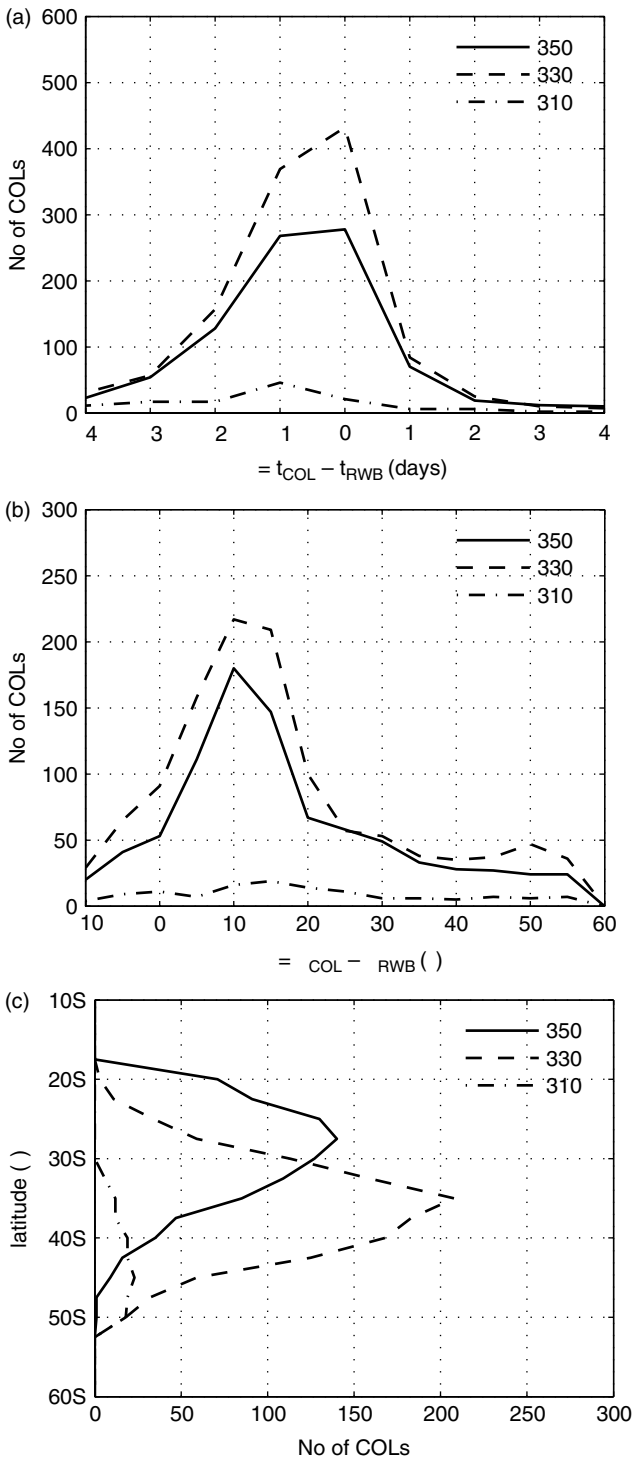

Figure 5. The distribution of COLs as a function of (a) time lag (days) between the occurrence of RWB and COLs ($= t_{COL}$ t_{RWB}), (b) the difference between the longitudes of the COLs and those of the associated RWB events (= COL RWB) and (c) latitude. The solid, dashed and dash-dotted curves represent frequency of occurrence of COL formation that are associated with RWB on the 350, 330 and 310 K isentropic surfaces, respectively.

3. Climatology of COLs

We first discuss the general climatological features of COLs at 250 hPa. A total of 3611 closed cyclonic circulations are identified at 250 hPa during the period 1979–2008, of which 2430 (81 COLs per year) comply with the cold-core condition and are classified as COLs. Geographical distributions of these systems (Figure 2) show that they occur in higher frequencies in the vicinity of the continents, and fewer are observed over the oceans, except over the western South Pacific (Fuenzalida *et al.*, 2005; Reboita *et al.*, 2009).

The 250 hPa COLs are prevalent during the summer (December to February, DJF) and are far less common during the wintertime (June to August, JJA) and early spring (September to November, SON) –Figure 3(a). This is consistent with studies at 200 hPa in the NH (e.g Kentarchos and Davies, 1998; Nieto *et al.*, 2005) and SH (Reboita *et al.*, 2009). We also applied the method of section 2.2 to the 200 hPa level and found that the seasonal and geographical distribution of COLs is similar to 250 hPa.

It is useful to divide the COLs into subtropical (20–35 S) and midlatitudinal (35–50 S) groups. This division is motivated by the fact that Kentarchos and Davies (1998) found that midlatitude COLs in the NH tend to have larger spatial scales and tend to be longer-lived than their subtropical counterparts. Figure 3(a) shows that subtropical systems at 250 hPa are more frequent than their midlatitude counterparts during SON and DJF, but the opposite is true during autumn (March to May, MAM) and winter (JJA) months.

There are important zonal variations in the occurrence of COLs, as shown in Figures 2(a) to (d), 3(c) and (e), for DJF and JJA. The seasonal variation of COLs is influenced most by the Australian/New Zealand sector (120 E–120 W). Here the COL frequency drops drastically from DJF to JJA. This is particularly true in the case of subtropical COLs. Note also that the midlatitude systems are extremely scarce over the ocean waters south of Africa and in the southern Indian Ocean (0–60 E) during DJF.

The variability in our climatology differs somewhat from that of Fuenzalida *et al.* (2005). We have also used our procedure to form a climatology of 500 hPa COLs (Figure 3(b)). In this climatology there is a total of 3761 closed circulations of which 2363 have a cold core. A similar plot to Figure 1 but for 500 hPa COLs (not shown) shows that the cold core occurs when six neighbouring grid points are warmer than the COL centre. The seasons when COLs are most frequent at 500 hPa differs from that at 250 hPa, i.e. the COLs at 500 hPa occur most frequently from MAM to SON and have their minimum count during DJF (Figure 3(b)). This shows that the difference in the variability found here (also in Reboita *et al.*, 2009) and in Fuenzalida *et al.* (2005) is because of the different levels considered and not the method. The reasons for the variation of COL seasonality with level will be examined further in section 4.3.

Although the frequency distributions of the 500 hPa COLs in our analysis are similar to those presented in Fuenzalida *et al.* (2005), we have identified significantly more COLs. There is better agreement with Fuenzalida *et al.* (2005) in the number of systems if we increase the number of grid points that are required to be warmer than the centre of the low to eight (Figure 1). This decreases the number of COLs to 1053 at 500 hPa, which corresponds to 5 COLs y ^{1} less than Fuenzalida *et al.* (2005), who found 40 COLs y ^{1}. The most likely reason for the discrepancies might that they implemented the cold core subjectively.

We have also identified five more COLs per annum than Reboita *et al.* (2009), but the interseasonal variability is in agreement with theirs. The reason for this difference might be that in their analysis they consider COLs that occur

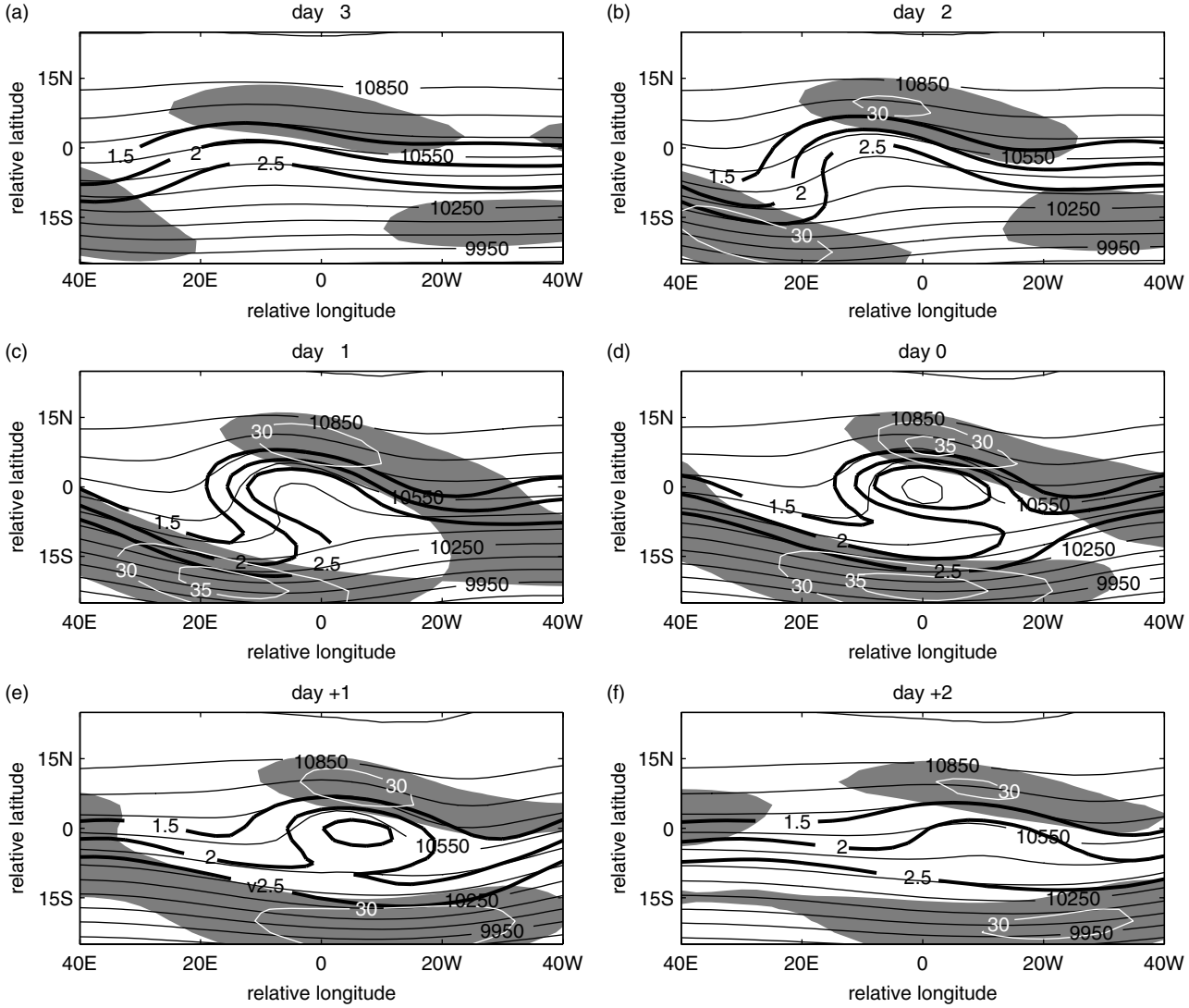

Figure 6. The evolution of composite mean fields from (a) three days before the formation of the COLs (day –3) to (f) two days after (day +2). The mean fields shown are geopotential heights at 250 hPa (thin contours with 100 gpm intervals), PV = –1.5, –2 and –2.5 PVU (bold contours), and jet streaks with wind speeds greater than 25 m s ^{1} (shading). White contours are isotachs beginning at 30 m s ^{1}. The composite mean fields were formed using COLs and RWB events that occur on the 330 K isentropic surface for = –1 day. The *x*- and *y*-axes represent the longitude and latitude axes relative to the centre of the COL pressure system.

during the pre-satellite era and show that their algorithm identifies fewer COLs during this period than from 1979 onwards. This is the case right through the SH, except in the Pacific Ocean.

4. Link between COLs and RWB

4.1. COL–RWB relationship

As discussed in the Introduction, the major focus of this study is to establish whether COLs can be linked to RWB in the SH. Thus, we first determine what percentage of the COLs can be linked to a RWB event. To find the link we proceed as follows. For every COL, we search for a RWB event that occurs 60 longitude upstream and 10 downstream of the COL centre, and occurs between four days prior to and four days after the day of the COL formation. We further require that the RWB event be within 15 latitude from the centre of the low.

Figure 4 shows an example of a COL pressure system (thin solid contours) with the cold core represented by the closed thickness (dotted) contour. The system began developing in the South Atlantic on 15 April 1985 and the closed circulation formed on 17 April 1985 with its centre at 40 S, 5 E. The closest RWB event to this particular COL that the search method identified occurred on 16 April 1985. Its position is represented by the westernmost point such that $_yPV < 0$ (section 2.3) on PV = –2 PVU (bold solid) contour on the 330 K surface at 50 S, 25 W. Note that in some cases a COL might have multiple RWB associations. In such situations the code chooses the RWB event closest to the COL in both space and time.

When applied to the 250 hPa COLs, the above procedure linked 2162 of 2430 (around 89%) COLs to a RWB event. In other words, the majority of the COLs are associated with RWB. The remaining 11% not linked to RWB are examined in the next section, however we note here that these COLs are actually linked to the equatorward advection of high-PV air but this advection of high-PV air does not meet the criteria for RWB described in the previous section.

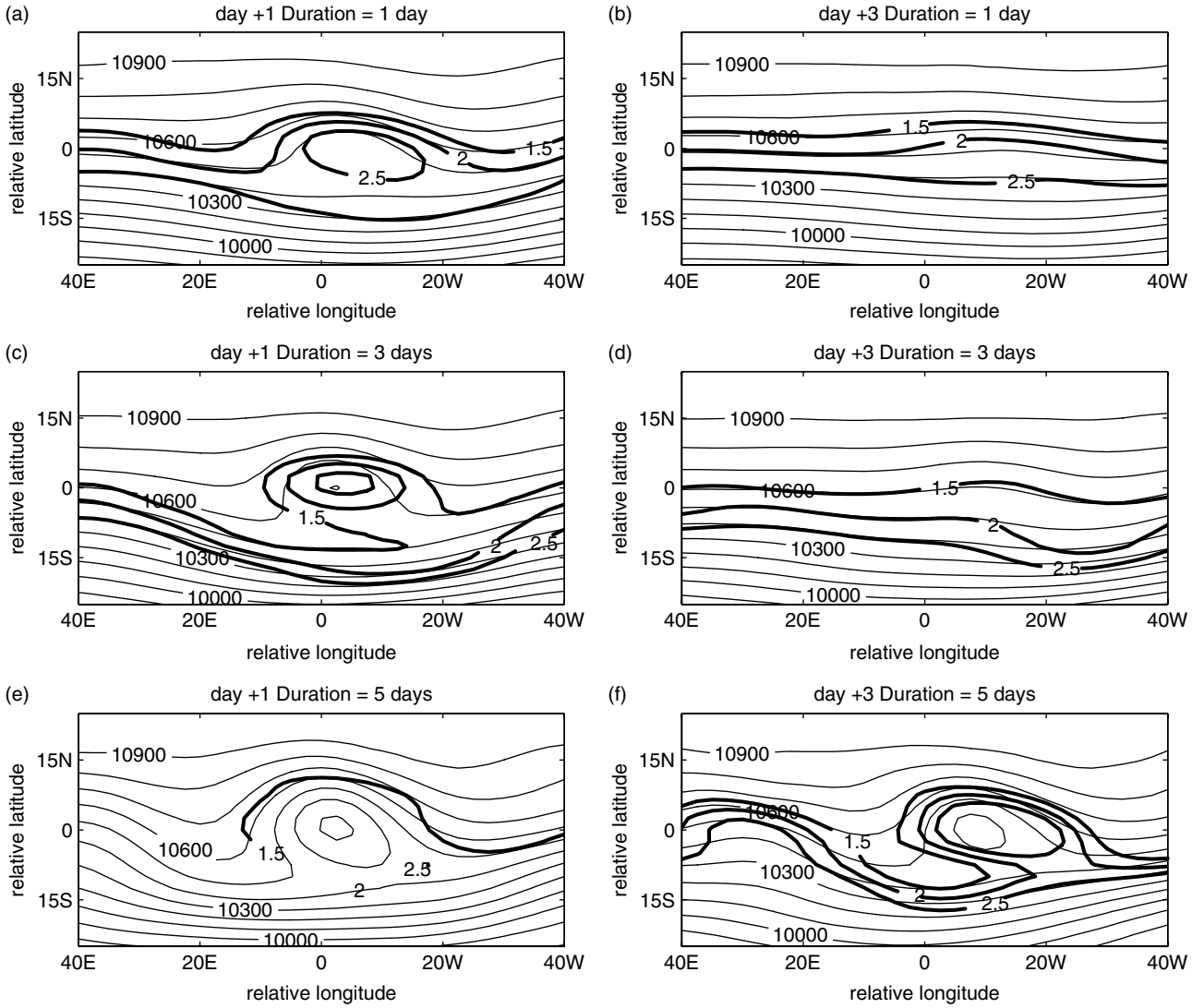

Figure 7. Composites of PV = –1.5, –2.0, –2.5 PVU (bold) contours and 250 hPa geopotential heights (thin contours) for 330 K COLs with 1-day duration and = 0, showing the COL development (a) one day (day +1) and (b) three days (day +3) after their formation. (c, d) and (e, f) are as (a, b), but for COLs with 3- and 5-day durations, respectively.

We focus in the remainder of this section on the 89% of COLs that can be linked to a RWB event. These COLs can be divided into three groups according to isentropic surfaces on which their associated RWB occur: 34%, 48% and 5% of the lows are associated with 350, 330 and 310 K RWB events, respectively. Hereafter, we will name the COLs according to their RWB associations; for example, COLs that are linked to RWB on the 350 K surface will be called '350 K COLs'.

The relative timing of COLs and RWB is shown in Figure 5(a), which shows the distribution of COLs as a function of time lag ($= t_{\mathrm{COL}}$ t_{RWB}, in days), with each group plotted separately. For nearly all of the COLs, the RWB events occur on or before the day the COLs form, with frequencies decreasing with increasing time lag (the vast majority of the lows form within two days of the breaking). Furthermore, almost all the RWB events occur upstream of the COLs with a large percentage of them occurring 0–20 west of the COLs (Figure 5(b)). This time lag and the position of RWB events relative to the COLs is consistent with the expectation that COLs are induced by high-PV anomalies (Hoskins *et al.*, 1985), and that the advection of high PV, and therefore RWB, precedes the formation of the COL.

This grouping of COLs by isentrope of accompanying RWB also tends to organize them latitudinally, with the COLs with a higher isentrope generally further north (Figure 5(c)). About 88% (70%) of 350 K (330 K) COLs occur north (south) of 35 S and are subtropical (midlatitude) systems. Therefore, there is overlap in the distributions across the demarcation latitude and so the categorising of the COLs in terms of the isentropic surface on which the associated RWB events occur is not the same as the subtropical versus midlatudinal classification. The reason for the spread of latitudes of the 330 and 350 K COLs is that the position of the dynamical tropopause changes with season (Liniger and Davies, 2004). This northward migration of the tropopause is most pronounced in the Australian region where the majority of the COLs form (Figure 2), just north of the split jet flow (Bals-Elsholtz *et al.*, 2001). Therefore some of the lows that are classified as subtropical in the usual sense are associated with RWB on the 330 K isentropic surface, when the dynamical tropopause has migrated north in winter. Similarly, some midlatitudinal systems are associated with 350 K RWB, particularly during the warmer months when the subtropical dynamical tropopause is at the southernmost position. Nonetheless this way of categorizing

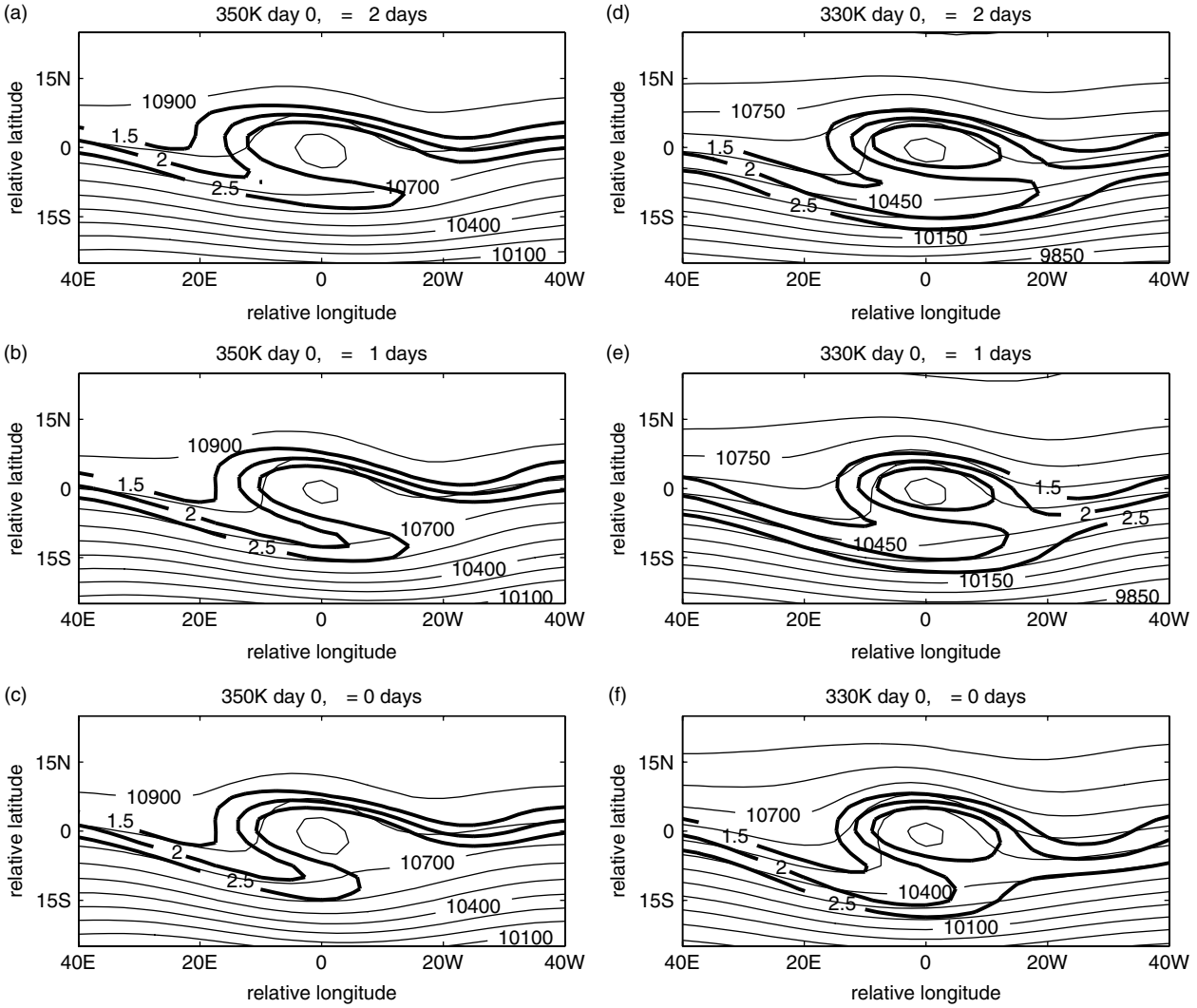

Figure 8. Composites of PV = –1.5, –2.0, –2.5 PVU (bold) contours and 250 hPa geopotential heights (thin contours with 100 gpm contour intervals) on day 0 on (a) 350 K and (b) 330 K COLs with = –2 days. (c, d) and (e, f) are as (a, b), but for = –1 day and = 0 days, respectively. The *x*- and *y*-axes represent the longitude and latitude axes relative to the centre of the COL pressure system.

COLs is considered more reliable because the variability and other characteristics of these systems are better explained in its context.

4.2. *Spatial structure*

We now examine the spatial structure of different fields during the evolution of the linked COLs and RWB. To do this, composite mean fields of all relevant fields are formed in the manner described in section 2.4. We show primarily composites that correspond to 330 K RWB and COLs with lag –1, but qualitatively similar results are found for all time lags and isentropic surfaces. The choice of presenting lag –1 instead of lag 0 is motivated by the desire to illustrate how RWB precedes COL formation as suggested above.

Figure 6 shows the evolution of 330 K PV, 250 hPa geopotential heights, and 'jet streaks' from day –3 (3 d before the formation of the COLs) to day +2 (2 d after they have formed). On day –3, the composites suggest that on average the Rossby waves propagate along the jet stream with a jet streak just southwest of where the PV contours appear to be undulating. The small amplitudes during the undulations suggest that nonlinear processes have not begun to take effect. As the jet streak moves eastward on day –2, the amplitude of the waves grows substantially and the undulations appear to have ceased because of the extensive deformation of the material contours, suggesting that nonlinearity is setting in.

By day –2 another important development is observed –the formation of the split jet flow (Holland *et al.*, 1987; Campetella and Possia, 2007). It appears that the formation of this flow regime is a result of the reduction in wind speeds where the PV contour deformation is most pronounced. The split flow structure consists of a larger, broader jet streak located southwest to southeast of the composite low and breaking event, and a smaller-scale jet streak north of the low pressure system. On day –1, the split jet is fully developed, the deformation of the PV contours is much more pronounced and there is now a region of reversed meridional PV gradients. This is the day on which the RWB actually occurs according to the definition used in this paper. As the Rossby waves break, high-PV air is advected onto the region of weak winds exactly where the COLs are anticipated to form.

The COLs form, by definition, on day 0. The closed isohypse characteristic of COLs is evident. At this time, the high-PV air has pinched off forming a closed high-PV

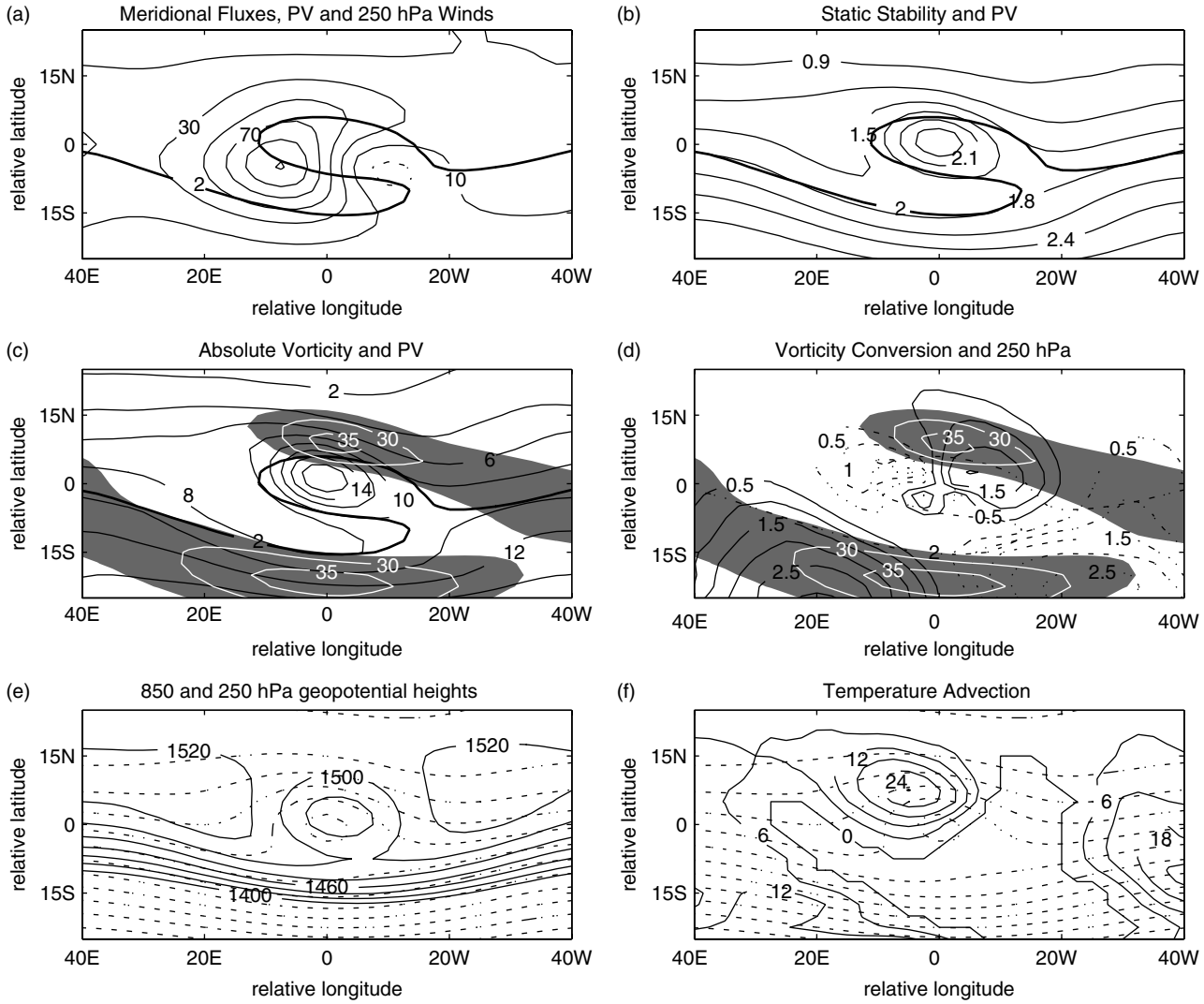

Figure 9. Composites for 330 K COLs corresponding to = –1 day on day 0: (a) meridional component of wave activity flux vector (thin solid and dashed contours with interval 15 $m^2 s^{-1}$) with PV = –2 PVU (bold) contour; (b) static stability, $_p$ (thin contours with interval 0.3 10^{-3} K Pa^{-1}); (c) absolute vorticity (thin contours with interval –2 10^{-5} s^{-1}); (d) conversion from shear to curvature vorticity (contours with interval 0.5 10^{-4} s^{-2}, solid for positive and dashed for negative); (e) geopotential heights at 850 hPa (solid) and 250 hPa (dashed) with interval 20 gpm; (f) cold advection at 850 hPa (solid contours with interval –6 10^{-6} K m s^{-1}), with geopotential heights at 250 hPa (dashed). In (c) and (d), wind speeds > 25 m s^{-1} are shaded with superimposed white isotachs at 5 m s^{-1} intervals.

anomaly. The anomaly persists until the next day and on day +2 it disappears. On day +1 the large jet streak continues to move eastward, and beyond day +2 (not shown) the split jet structure is destroyed. All the while, the northern component of the split jet has been somewhat stagnant and starts dissipating from day +2.

This analysis involves all COLs and does not take their duration into consideration. For this reason, the COL signal disappears completely on day +1 because most of the systems are short-lived (e.g. Fuenzalida *et al.*, 2005; Nieto *et al.*, 2005; Reboita *et al.*, 2009) with 58%, 25% and 10% lasting 1, 2 and 3 d respectively. However, if the longevity of the systems is considered, then the signal becomes evident beyond day 0. For example, for COLs that persist for 3 and 5 d, it can be observed on day +1 (Figure 7(c) and (d)) and day +3 (Figure 7(e) and (f)), respectively. The longer-lived COLs are maintained by the persistent high-PV anomaly (Hoskins *et al.*, 1985).

The evolution and structure of the PV and geopotential height fields is very similar for the composites of COLs with other time lags between RWB and the COL, and for RWB on the 350 K surface. This is illustrated in Figure 8 showing the composite fields at day 0 for different time lags and isentropic surfaces. The geopotential height fields show that the 330 K COLs are larger and deeper than their 350 K counterparts. A comparison of the evolution of the associated 350 K and 330 K PV suggests that the 330 K PV anomaly is more persistent and therefore 330 K COLs are longer-lived (Hoskins *et al.*, 1985). This is consistent with the findings of Kentarchos and Davies (1998) in the NH.

Note also that the distortion of the PV contours occurs on the equatorward side of the jet and is therefore influenced by anticyclonic shear. The waves consequently break in an anticyclonic fashion, as shown in Peters and Waugh (2003) using simple barotropic shear arguments. The deformed PV contours have a northwest–southeast tilt (Thorncroft *et al.*, 1993; Lee and Feldstein, 1996), signalling this anticyclonic breaking which is confirmed by the equatorward direction of the meridional fluxes of wave activity that have been shown in previous studies to be associated with anticyclonic

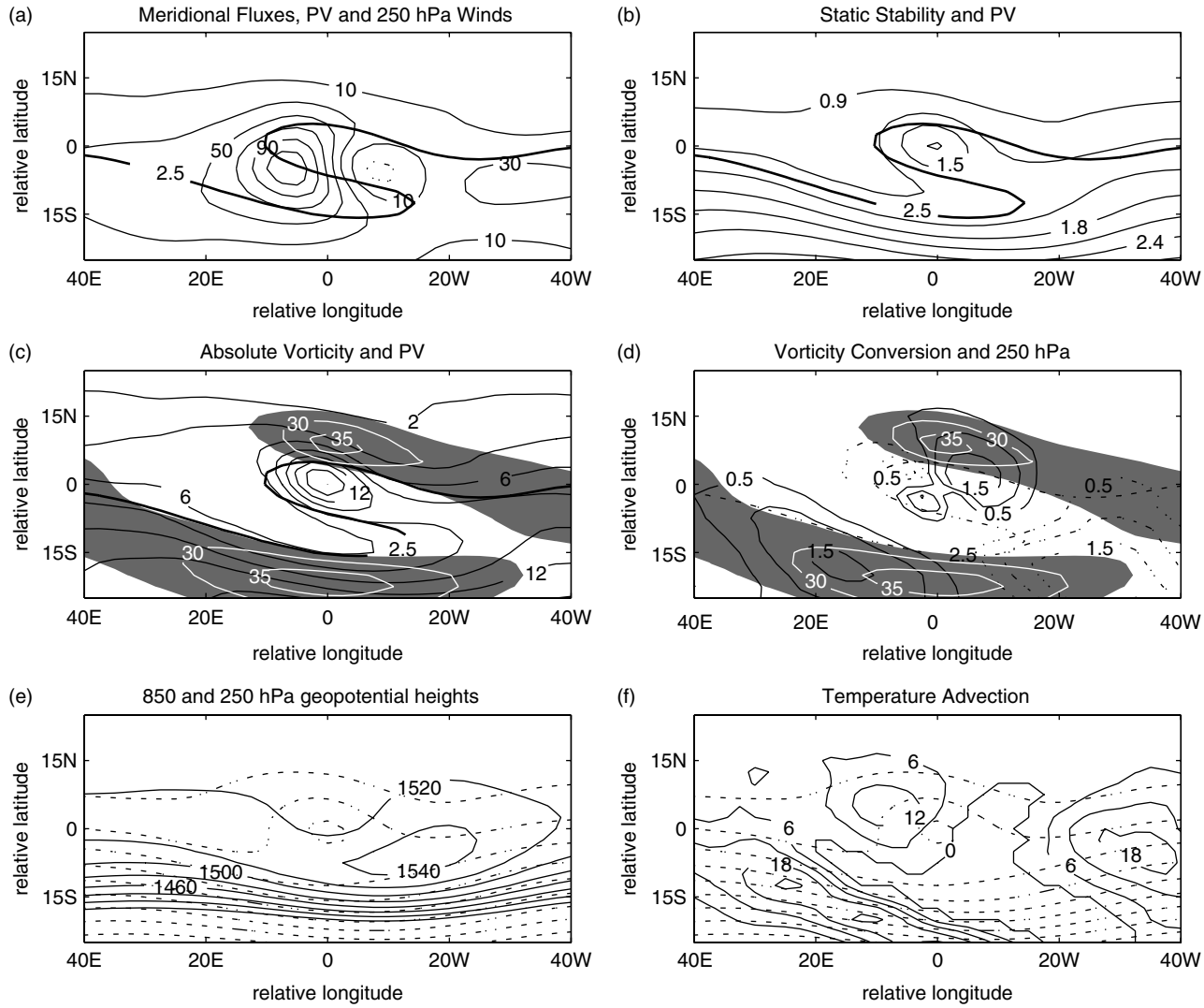

Figure 10. As Figure 9, but for 350 K COLs.

RWB, as shown in Figure 9(a) (e.g. Esler and Haynes, 1999; Gabriel and Peters, 2008).

The above composite analysis confirms that COL formation in the SH is strongly associated with anticyclonic RWB and the equatorward advection of high PV occurring on the equatorward lobe of the RWB. It is also of interest to examine the evolution of other fields during the RWB and formation of COLs. As described in Hoskins *et al.* (1985), PV anomalies appear as a combination of anomalies of absolute vorticity and static stability. Next, we examine the composite fields of these two fields.

First consider the static stability (e.g. Trenberth, 1991) shown in Figure 9(b). The anomalies in this quantity are clearly caused by the advection of high static stability stratospheric air into the troposphere during the RWB process. Secondly, as the waves are breaking, absolute vorticity anomalies form on the area where the COLs form (Figure 9(c)). Absolute vorticity can be written in terms of curvature and shear vorticity (Holton, 2004). These two forms of vorticity play a crucial role in establishing absolute vorticity fields in COLs by converting from one form to the other (Bell and Keyser, 1993). In the NH, the conversions are facilitated by the presence of a jet streak that propagates along the periphery of the amplifying trough (Keyser and Shapiro, 1986; Bell and Keyser, 1993). However, the above composites seem to suggest that the evolution of wind fields differs from the NH. In the SH a split flow forms, and its quasi-stationary northern component appears to be the one that facilitates the conversions. This is confirmed by Figure 9(d), showing the conversion terms on day 0, calculated using the expressions in the appendix of Bell and Keyser (1993). Using the vorticity sign convention of the SH, positive values (solid) mean conversions from shear vorticity to curvature vorticity and the negative (dashed) ones mean the reverse conversion. Shear vorticity is converted to curvature vorticity at the right exit of the northern component of the split jet and curvature vorticity is converted to its shear counterpart at the jet streak right entrance. The static stability anomalies, the split jet, and hence the absolute vorticity anomalies, all form as the waves are breaking and not before, which suggests that the RWB plays a role in establishing conditions conducive for COL formation aloft. These arguments apply at the 350 K surface as confirmed by Figures 10(a) to (d).

Upper-level PV processes also affect surface development (Hoskins *et al.*, 1985). We therefore investigate the surface conditions of COLs linked to RWB occurring on different surfaces. Figures 9(e) and 10(e) show 850 hPa (solid) and 250 hPa (dashed) geopotential heights, for composites for

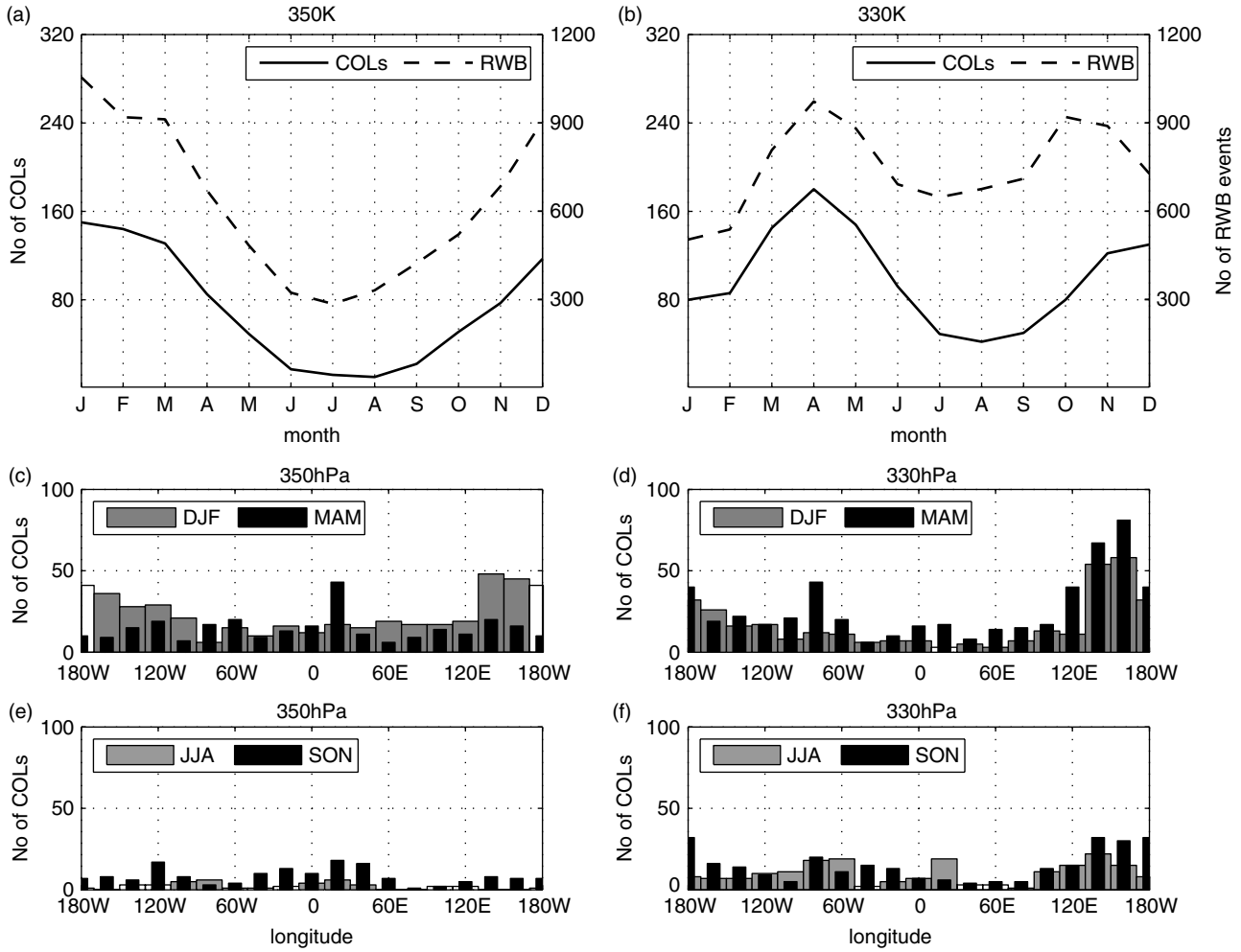

Figure 11. Frequency of RWB (dashed) and COLs (solid) as a function of month. The left and right *y*-axes represent the number of COLs and RWB events, respectively. (a) is for RWB on the 350 K isentropic surface and the COLs that are associated with them. (b) is as (a) but for RWB on the 330 K surface. (c) is the distribution of COLs associated with RWB on the 350 K isentropic surface as a function of longitude for DJF and MAM. (d) is as (c) but for COLs that are associated with RWB on the 330 K isentropic surface. (e, f) are as (c, d) but for JJA and SON.

330 K and 350 K COLs, respectively. Although the upper-level evolution is similar, the evolution of the 850 hPa geopotential heights differs between the 350 K and 330 K composites. 350 K COLs are associated with a north–south trough–ridge system, whereas the surface low for 330 K COLs develops between two high pressure systems located east and west of it. The different development patterns are similar with differences in case-studies for COLs over the land and ocean. Synoptic structures similar to the 350 K composites have been observed over South Africa (Taljaard, 1985) and were presented schematically by Holland *et al.* (1987) and Katzfey and McInnes (1996), whereas development similar to the 330 K composites have been observed for case-studies of ocean COLs (e.g. Taljaard, 1985; Figure 3 of Katzfey and McInnes, 1996).

It is expected that there will be cold advection associated with COL formation. The composite surface temperature advection $T_A = \mathbf{v} \cdot T$, where $\mathbf{v}$ and T are horizontal velocity and temperature respectively, for the 330 K and 350 K COLs are shown in Figures 9(f) and 10(f), respectively. In the case of 350 K COLs, cold fronts usually precede the eastward ridging high pressure systems (Figure 10(e) solid contours), as seen for example south of South Africa (Taljaard, 1985). The cold advection caused by the cold fronts deepens the upper-level developing troughs and COLs form eventually. In both these scenarios, the cold advection is concentrated over the northwestern portion of the deepening upper-level trough. However, cold advection associated with 350 K COLs is weaker than that associated with 330 K systems, which is consistent with deeper 330 K COLs than their 350 K counterparts (Figure 8). This occurs because cold fronts associated with Figure 10(e) make their passage much earlier prior to the ridging of the high.

In summary, the evolution of the PV, geopotential height, static stability, vorticity and temperature advection fields for COL-based composites are consistent with theoretical expectations (e.g. Hoskins *et al.*, 1985). The high-PV anomalies are established before the formation of COLs by RWB processes that precede them. The anomalies then induce the closed circulations. By the hypsometric relation, temperature advection at the surface reduces temperature in the column of air immediately above it, thereby creating the cold core.

4.3. *Influence of RWB on COL variability*

The above link between RWB and COLs provides a possible way of connecting the variability of COLs to that of jet streams in the SH. Several previous studies have

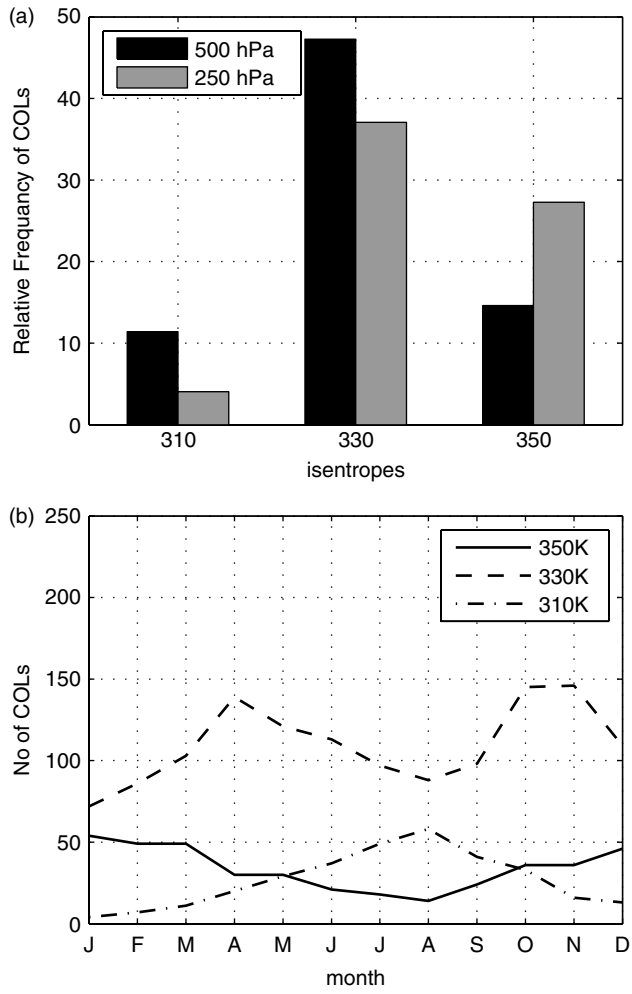

Figure 12. (a) The relative frequency of 500 hPa (black) and 250 hPa (grey) COLs as a function of isentropic surface on which the RWB occurs with which they are associated. (b) Frequency of COLs at 500 hPa that are associated with RWB on the 350 K (solid), 330 K (dashed) and 310 K (dash-dotted) isentropic surfaces, as a function of month.

linked RWB and jet variability in the SH (e.g. Postel and Hitchman, 1999; Berrisford *et al.*, 2007), and can be used to understand variability in COLs which will be explained using Figure 11.

Figures 11(a) and (b), for the 350 and 330 K isentropic surfaces respectively, show the variation of RWB events (dashed) on the right y-axis. The left y-axis shows the variability of COLs (solid) that are associated with RWB events on the respective isentropic surfaces. Figures 11(c) and (e) show the longitudinal variation of 350 K COLs; Figures 11(d) and (f) are similar but for 330 K COLs.

The subtropical and polar front jets (STJ and PFJ), as waveguides (e.g. Hoskins and Ambrizzi, 1993; Ambrizzi *et al.*, 1995), restrict the meridional growth of wave amplitude and therefore inhibit the RWB process. The waves break more often when they propagate in reduced zonal wind speeds (Peters and Waugh, 1996; Swanson *et al.*, 1997). Because COLs are linked to RWB, it is then plausible that the seasonal march of the jets will influence the interseasonal variability of COLs on both isobaric surfaces, by first influencing that of RWB. Indeed, the similarities between seasonal profiles (Figures 11(a) and (b)) of these processes support this notion.

To understand this further, the COLs are broken down into seasonal longitudinal variations according to their RWB links on various surfaces. As was the case with subtropical lows (Figure 3(c)), the Australian/New Zealand sector plays the most significant role in influencing 350 K COL occurrence around 30 S or so (Figures 11(c) and (e)), as the reduction of these COLs from DJF to JJA is clear. The reason for this is that 350 K RWB is inhibited by the STJ during JJA because this jet is a waveguide for these waves during this season and so RWB events induce fewer COLs. There are changes in other subtropical regions but they are not as significant because the STJ is not strong there (Hurrell *et al.*, 1998).

The hemispheric-wide increases in 330 K COLs from DJF to MAM (Figure 11(d)) are caused by the fact that the PFJ ceases being a waveguide as RWB activity and the dynamic tropopause migrates equatorward (Figures 2(a) and (b)). These increases are also evident in Figure 11. Moreover, 330 K COLs break in the reduced zonal flow of the split jet structure (Bals-Eslholz *et al.*, 2001). Figures 11(d) and (f) show that away from the STJ region there are increases in COL counts from MAM to JJA, however modest, whilst there are reductions in the Australian sector. The latter is caused by the fact that the 330 K dynamical tropopause has migrated into the STJ (Figure 2), north of the weak flow of the split jet, which tends to reduce 330 K RWB events and hence 330 K COLs there. Increases in COL occurrence from JJA to SON is associated with the southward migration of the dynamical tropopause and the dissipation of the STJ. Therefore the variability of the jet streams in the SH regulates the seasonal occurrence of COLs at 250 hPa, by first influencing the interseasonal variations in RWB occurrence. Note that the STJ reduces COLs more significantly than the PFJ at this level.

The variability of the jet streams and of RWB can be used to understand the differences in the interseasonal variability of COLs at 250 hPa and 500 hPa. 81% of the 500 hPa COLs are linked to RWB. Therefore arguments similar to those above apply, but note that Figure 12(a) shows that RWB at 310 and 330 K make a larger contribution to COLs at 500 hPa. Consequently these RWB events will play a more significant role in inducing COLs at 500 hPa than 350 K RWB events. This is particularly true in JJA as shown in Figure 12(b). On this basis, the PFJ reduces 500 hPa COLs more effectively during DJF than those at 250 hPa and the STJ does not affect the COLs at 500 hPa as much as at the higher level, as discussed above.

5. COLs with no RWB association

As discussed in section 4, 11% 250 hPa of COLs identified in the SH do not have any RWB association. We now consider these systems. 51% (49%) of these COLs occur in the Subtropics (midlatitudes), where 35 S is used to separate subtropical and midlatitudinal systems as before. To analyse their structure and their possible relationship with isentropic PV processes, their composites with PV on 350 and 330 K surfaces are then formed in the same way as before.

The composite mean fields show that the PV anomaly that is associated with the closed cyclonic circulation of these COLs is due to the equatorward advection of stratospheric air. Figure 13 shows the deformation of material contours which does not satisfy the RWB criteria used in this paper

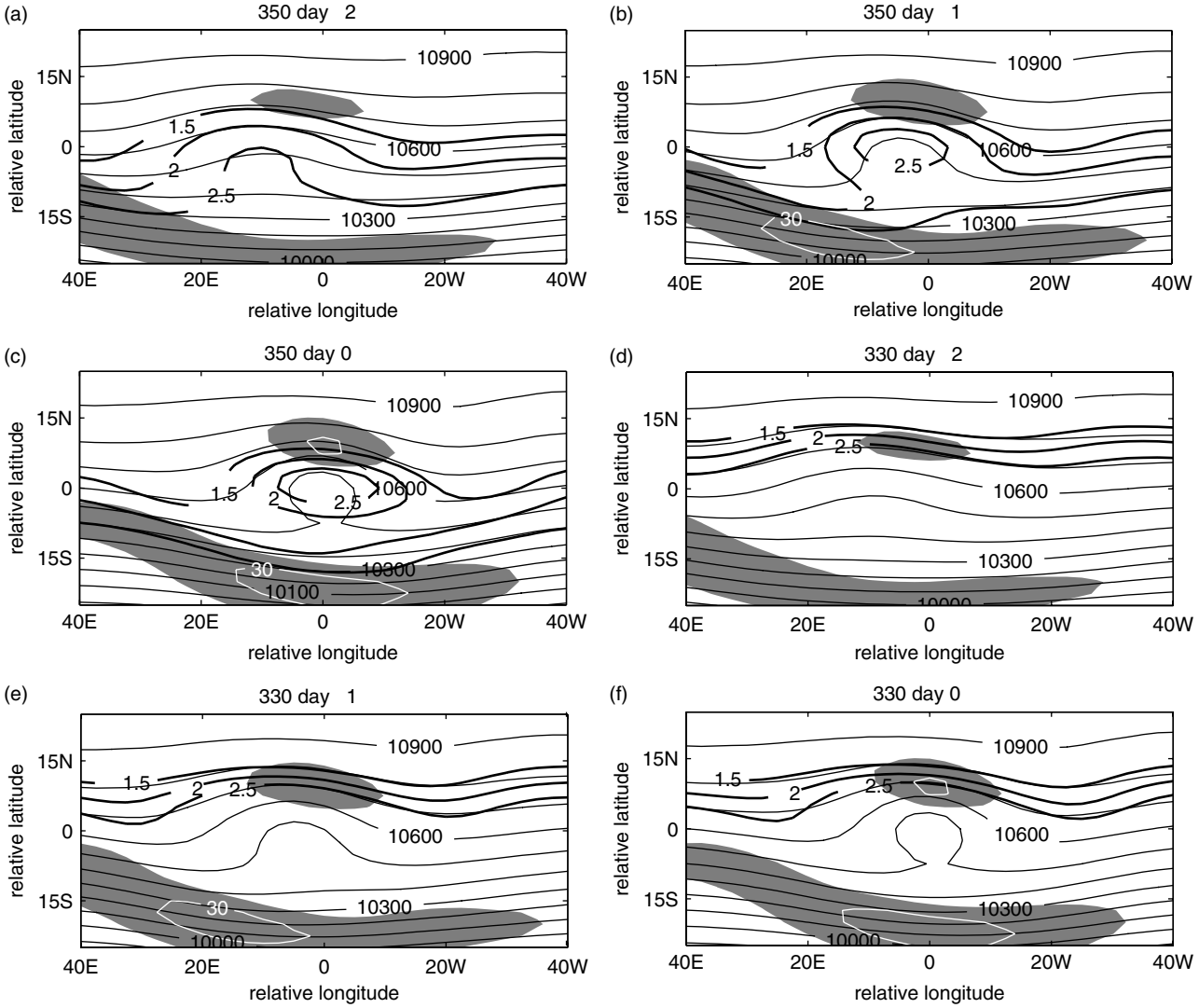

Figure 13. The composite evolution of geopotential heights at 250 hPa (thin black contours with interval 100 gpm) together with PV intrusions (bold black contours at –1.5, –2.0 and –2.5 PVU) on the (a) 350 K and (b) 330 K isentropic surfaces. The evolution of the fields is from (a, b) two days before the formation of the COLs (day –2) to (e, f) the day of their formation (day 0). The shaded regions denote wind speeds $> 25\,\mathrm{m\,s^{-1}}$ and the white contours are isotachs beginning at $30\,\mathrm{m\,s^{-1}}$. The x- and y-axes represent the longitude and latitude axes relative to the centre of the COL pressure system.

because there is very weak overturning, or no overturning at all. We refer to such events as 'PV intrusions'. Such processes have been studied in the Tropics (e.g. Waugh and Polvani, 2000) and have been found to induce localised convection (e.g. Waugh and Funatsu, 2003; Funatsu and Waugh, 2008).

Unlike RWB, the advection of stratospheric air during a PV intrusion process has a north–south orientation that is mostly neither cyclonic nor anticyclonic, but can be weakly anticyclonic. Figure 14(a) confirms this to be the case because the meridional fluxes of wave activity are almost equally poleward as they are equatorward and their positions relative to each other is suggestive of equatorward advection of air. Furthermore, the PV anomalies appear as a combination of the static stability and vorticity anomalies, and the northern jet streak facilitates the vorticity conversion as previously discussed (Figures 14(b), (c), and (d)). Surface geopotential height structures (Figures 14(e) and (f)) suggest that the influence of 330 K PV intrusions on the these COLs dominates over that of the 350 K intrusions. This is consistent with Figure 13 which shows stronger PV anomalies on the 330 K surface than at 350 K.

PV intrusions, like RWB, involve the meridional growth of wave amplitude. Therefore they too can be inhibited by the waveguides but are enhanced in weak zonal flow as found by Waugh and Polvani (2002) in the Tropics. COLs associated with them can therefore be expected to be minimized near jet cores and enhanced in diffluent and confluent flow. Therefore, in a similar manner to RWB, jet variability first influences the occurrence of the intrusions, which in turn influences the rates at which the COLs are induced.

6. Summary and conclusions

Using 30 years of NCEP/NCAR reanalysis of data, a climatology of COLs has been formed and the link between the COLs and RWB, and to a lesser extent PV intrusions, has been established in the SH. COLs at 250 hPa level occur most frequently during the summer and much less during the winter, which is consistent with studies in the NH at 200 hPa (e.g. Kentarchos and Davies, 1998; Nieto *et al.*, 2005) and SH (Reboita *et al.*, 2009). In contrast, 500 hPa COLs occur more frequently during the colder months

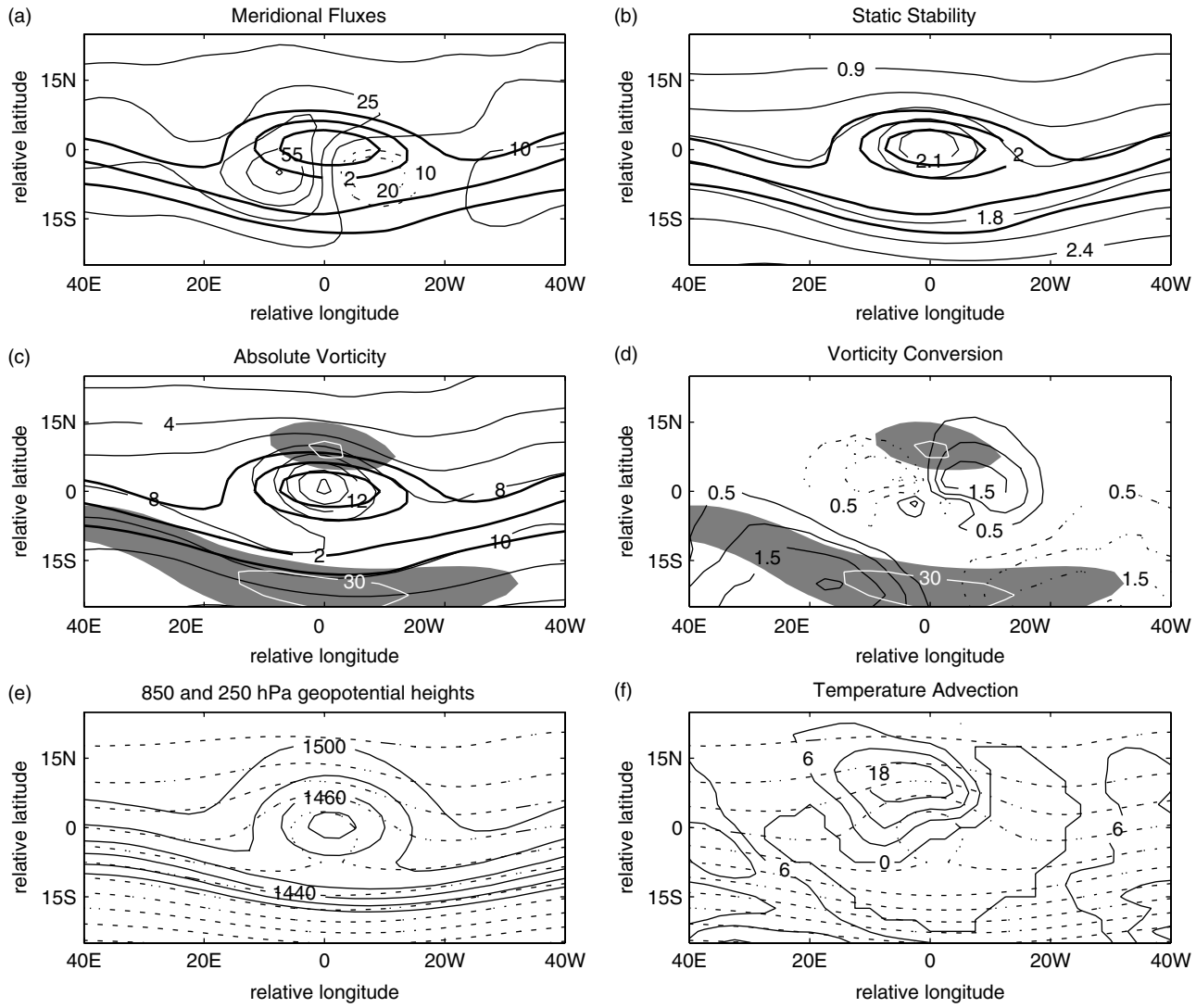

Figure 14. As Figure 9, but for PV intrusions.

than during the summer, consistent with Fuenzalida *et al.* (2005).

It was found that 89% of COLs in the SH have an associated RWB event and the remaining 11% of COLs are linked to PV intrusions. Most of the RWB events precede or occur on the same day as the COL and occur upstream of the COLs. This timing and position of the RWB relative to the COLs suggests that the relationship between these two processes might have implications for the predictability of the COLs. Furthermore, these statistics confirm the assertion made by Price and Vaughan (1993) that COLs and tropopause folds accompany one another.

Analysis of the evolution of COL events showed that
(1) the split jet known to be associated with COLs in the SH (e.g. Holland *et al.*, 1987) forms as the Rossby waves break and that its northern component facilitates the shear-curvature vorticity conversions (Bell and Keyser, 1993) which establish the absolute vorticity anomaly where the COLs form, and
(2) the RWB process is responsible for the anticyclonic advection of stratospheric air that causes the static stability anomaly.
Both these processes occur prior to the formation of the COL and their combination creates a high-PV anomaly field which in turn induces the COL, in keeping with theoretical expectations (Hoskins *et al.*, 1985).

The evolution of the COLs associated with 330 and 350 K RWB reveal that the PV anomalies associated with the former are more persistent, stronger and have a larger spatial scale than those associated with the latter. Although the structure aloft is similar, surface processes associated with 350 and 330 K COLs are dissimilar. For 350 K COLs, a surface trough with a ridging high south of the trough is evident. This structure is also seen in Holland *et al.* (1987) and was also discussed by Taljaard (1985). In contrast, 330 K COLs are associated with a closed surface low flanked by two high pressure systems east and west of it. Both these structures have the ability to facilitate the passage of cold fronts. In the 350 K case, the fronts pass much earlier than the formation of the COL, resulting in weaker cold advection at the time of COL formation than in the 330 K case. As a result, 330 K COLs are deeper than 350 K COLs.

Intrusions on the 330 K surface appear to dominate over those on the 350 K surface in their influence on the 11% of COLs that have no RWB association. The surface conditions of the systems are similar to those of COLs associated with RWB on the 330 K surface.

The similarity between the seasonal profiles of 350 K and 330 K COLs and the RWB events on these surfaces and

the occurrence of RWB before COLs suggest that RWB interseasonal variations influence those of COLs. Previous studies have shown that RWB variability is influenced by jet variability (e.g. Postel and Hitchman, 1999; Berrisford *et al.*, 2007), implying that jet variability influences COLs seasonality in the SH. More specifically, the subtropical jet reduces COLs in the Subtropics from summer to winter in the Australian–west South Pacific region and the polar front jet keeps COL frequencies to a minimum in summer in the midlatitudes in particular over the Southern Ocean and south Indian Ocean waters.

The association of 500 hPa COLs with RWB shows that the subtropical jet has a less adverse effect on these systems than their 250 hPa counterparts and the polar front jet plays a more significant role in inhibiting COLs at 500 hPa than those at 250 hPa. This explains the differences in seasonal variations of COLs between 250 and 500 hPa.

Although we have shown that COLs are linked to RWB or PV intrusions, it is important to note that there are many more RWB events than COLs or closed circulations. In fact, only 9% (12%) of RWB events produce COLs (closed circulations). This raises the important question of why some RWB events produce COLs but others do not. Preliminary analysis shows that the average PV anomaly is larger in RWB events that produce COLs. However, there are still many RWB events with large PV anomalies that do not produce COLs, suggesting that whether COLs are produced is not simply dependent on the strength of PV anomalies produced during the RWB. It is likely that the ambient flow conditions are a major factor in whether COLs are produced.

Furthermore, the duration of the COLs has not been considered in this study, as we focus on the inception of COL systems relative to that of RWB. Since the re-intensification of COLs involves, in part, the injection of high-PV air (Hoskins *et al.*, 1985; Price and Vaughan, 1993), the RWB process is envisaged to play a role in their maintenance. These issues will be examined in a future study.

Acknowledgements

This work was funded by the US National Science Foundation and the South African National Research Foundation. The authors would like to thank Mary-Jane Bopape, Chang Lang, Isaac Ngwana, Raquel Nieto, Luke Oman, Dieter Peters and the two anonymous reviewers for helpful comments that assisted in improving the manuscript.

References

Ambizzi T, Hoskins BJ, Hsu H. 1995. Rossby wave propagation and teleconnection patterns in the Austral winter. *J. Atmos. Sci.* **52**: 3661–3762.

Ancellet G, Beekmann M, Papayannis A. 1994. Impact of a cut-off lows development transport of ozone in the free troposphere. *J. Geophys. Res.* **99**(D2): 3451–3468.

Appenzeller C, Davies HC. 1992. Structure of stratosphere intrusions into the troposphere. *Nature* **358**: 570–572.

Appenzeller C, Davies HC, Norton WA. 1996. Fragmentation of stratospheric intrusions. *J. Geophys. Res.* **101**(D1): 1435–1956.

Baldwin MP, Holton JR. 1988. Climatology of the stratospheric polar vortex and planetary wave breaking. *J. Atmos. Sci.* **45**: 1123–1142.

Bals-Elsholz TM, Atllah EH, Bosart LF, Wasula TA, Cempa MJ, Lupo AR. 2001. The wintertime Southern Hemisphere split: Structure, variability and evolution. *J. Climate.* **14**: 4191–4215.

Baray JL, Baldy S, Diab RD, Cammas JP. 2005. Dynamical study of a tropical cut-off low over South Africa and its impact on tropospheric ozone. *Atmos. Env.* **37**: 1475–1488.

Barsby J, Diab RD. 1995. Total ozone and synoptic weather relationships over southern Africa and surrounding oceans. *J. Geophys. Res.* **100**(D2): 3023–3032.

Bell GD, Keyser D. 1993. Shear and curvature vorticity and potential-vorticity interchanges: Interpretation and application to a cut off cyclone event. *Mon. Weather Rev.* **121**: 76–102.

Berrisford P, Hoskins BJ, Tyrlis E. 2007. Blocking and Rossby wave breaking on the dynamical tropopause in the Southern Hemisphere. *J. Atmos. Sci.* **64**: 2881–2898.

Campetella CM, Possia NE. 2007. Upper-level cut-off lows in southern South America. *Meteorol. Atmos. Phys.* **96**: 181–191.

Edouard S, Vautard R, Brunet G. 1997. On the maintenance of potential vorticity in isentropic coordinates. *Q. J. R. Meteorol. Soc.* **123**: 2069–2094.

Elser JG, Haynes PH. 1999. Baroclinic wave breaking and the internal variability of the tropospheric circulation. *J. Atmos. Sci.* **56**: 4014–4031.

Fuenzalida HA, Sanchez R, Garreaud RD. 2005. A climatology of cutoff lows in the Southern Hemisphere. *J. Geophys. Res.* **110**: D181001, DOI: 10.1029/2005JD005934.

Funatsu BM, Waugh DW. 2008. Connections between potential vorticity intrusions and convection in the Eastern Tropical Pacific. *J. Atmos. Sci.* **65**: 987–1002.

Gabriel A, Peters D. 2008. A diagnostic study of different types of Rossby wave breaking in the northern extratropics. *J. Meteorol. Soc. Japan.* **86**: 613–631.

Hitchman MH, Huesmann AS. 2007. A seasonal climatology of Rossby wave breaking in the 320–2000 K layer. *J. Atmos. Sci.* **64**: 1922–1940.

Holland GJ, Lynch AH, Leslie LM. 1987. Australian east-coast cyclones Part 1: Synoptic overview and case study. *Mon. Weather Rev.* **115**: 3024–3026.

Holton JR. 2004. *An Introduction to Dynamic Meteorology.* Elsevier Academic Press:.

Hoskins BJ, Ambrizzi T. 1993. Rossby wave propagation on a realistic longitudinal varying flow. *J. Atmos. Sci.* **50**: 1661–1671.

Hoskins BJ, McIntyre ME, Robertson AW. 1985. On the use and significance of isentropic potential vorticity maps. *Q. J. R. Meteorol. Soc.* **111**: 877–946.

Hurrell JW, van Loon H, Shea DJ. 1998. The mean state of the troposphere. In *Meteorology of the Southern Hemisphere. Meteorol. Monogr.* **49**: 1–46.

Kalnay E, Kamitsu M, Kistler R, Collins W, Deaven D, Gandin L, Iredell M, Saha S, White G, Woolen J, Zhu Y, Cheliah M, Ebisukazi W, Higgins W, Janowiak J, Mo KC, Ropelewski C, Wang W, Leetmaa A, Reynolds R, Jenne R, Joseph D. 1996. The NCEP/NCAR 40-year reanalysis project. *Bull. Amer. Meteorol. Soc.* **77**: 437–471.

Katzfey JJ, McInnes KL. 1996. GCM simulations of eastern Australian cutoff lows. *J. Climate.* **9**: 2337–2355.

Kentarchos AS, Davies TD. 1998. A climatology of cut-off lows at 200 hPa in the Northern Hemisphere, 1990–1994. *Int. J. Climatol.* **18**: 379–390.

Keyser D, Shapiro MA. 1986. A review of the structure and dynamics of upper-level frontal. *Mon. Weather Rev.* **144**: 452–499.

Kistler R. Kalnay E, Collins W, Saha S, White G, Woollen J, Chelliah M, Ebisukazi W, Kanamitsu, Kousky V, van den Dool H, Jenne R, Fiorino M. 2001. The NCEP-NCAR 50-year reanalysis: Monthly means CD-ROM and documentation. *Bull. Amer. Meteorol. Soc.* **82**: 247–267.

Langford AO, Masters CD, Proffitt MH, Hsie E-Y, Tuck AF. 1996. Ozone measurements in a tropopause fold associated with a cut-off low system. *Geophys. Res. Lett.* **23**(18): 2501–2504.

Lee S, Feldstein S. 1996. Two types of wave breaking in an aquaplanet GCM. *J. Atmos. Sci.* **53**: 842–857.

Liniger MA, Davies HC. 2004. Seasonal differences in extra-tropical potential vorticity variability at tropopause levels. *J. Geophys. Res.* **109**: D117102, DOI: 10.1029/2004JD004639.

Mastumoto SK, Ninomiya K, Hasegawa R, Miki Y. 1982. The structure and and role of a subsynoptic cold vortex on the heavy precipitation. *J. Meteorol. Soc. Japan* **60**: 339–353.

McIntyre ME, Palmer TN. 1983. Breaking planetary waves in the stratosphere. *Nature* **305**: 593–600.

Nieto R, Gimeno L, De La Torre L, Ribera P, Gallego D, García-Herrera R, García JA, Munez M, Redano A, Jerónimo L. 2005. Climatological features of cutoff low systems in the Northern Hemisphere. *J. Climate* **18**: 3085–3103.

Nieto R, Sprenger M, Wernli H, Trigo RM, Gimeno L. 2008. Identification and climatology of cut-off lows near the tropopause. In *Trends and directions in climate research. Ann. N.Y. Acad. Sci.* **1146**: 256–290.

Oltmans S, Levy II H, Harris JM, Merrill Jt, Moody JL, Lathrop J, Cuevas E, Trainer M, O'Neill MS, Prospero JM, Vömel H, Johnson BJ. 1996.

Summer and spring ozone profiles over the the North Atlantic from ozonesonde measurements. *J. Geophys. Res.* **101**(D22): 29179–29200.
Palmén E, Newton CW. 1969. *Atmosphere Circulation Systems: Their Structure and Physical Interpretation.* Academic Press: New York.
Peters D, Waugh DW. 1996. The influence of barotropic shear on the poleward advection of upper tropospheric air. *J. Atmos. Sci.* **53**: 3013–3031.
Peters D, Waugh DW. 2003. Rossby wave breaking in the Southern Hemisphere wintertime upper troposphere. *Mon. Weather Rev.* **131**: 2623–2634.
Postel GA, Hitchman MH. 1999. A climatology of Rossby wave breaking along the subtropical tropopause. *J. Atmos. Sci.* **56**: 359–373.
Price JD, Vaughan G. 1993. The potential for stratosphere-troposphere exchange in cut-off low systems. *Q. J. R. Meteorol. Soc.* **119**: 343–365.
Qi L, Leslie LM, Zhao SX. 1999. Cut-off low pressure systems over southern Australia: Climatology and case study. *Int. J. Climatol.* **19**: 1633–1649.
Reboita MS, Nieto R, Gimeno L, da Rocha RP, Ambrizzi T, Garreaud R, Krüger LF. 2009. Climatological characteristics of cut-off low systems in the Southern Hemisphere. *J. Geophys. Res.* in press.
Singleton AT, Reason CTC. 2007. Variability in the characteristics of cut-off low pressure systems over subtropical southern Africa. *Int. J. Climatol.* **27**: 295–310.
Swanson KL, Kushner PJ, Held IM. 1997. Dynamics of barotropic storm tracks. *J. Atmos. Sc.* **54**: 791–810.
Taljaard JJ. 1985. *'Cut-off lows in the South African region'*. Tech. Paper 14. South African Weather Service: Pretoria, RSA.
Tennant W. 2004. Consideration when using pre-1979 NCEP/NCAR reanalysis in the Southern Hemisphere. *Geophys. Res. Lett.* **31**: L11112, DOI: 10.1029/2004GL019751.
Thorncroft CD, Hoskins BJ, McIntyre ME. 1993. Two paradigms of baroclinic-wave life cycle behaviour. *Q. J. R. Meteorol. Soc.* **119**: 17–55.
Trenberth KE. 1991. Storm tracks in the Southern Hemisphere. *J. Atmos. Sci.* **48**: 2159–2178.
van Delden A, Neggers R. 2003. A case study of tropopause cyclogenesis. *Meteorol. Appl.* **10**: 187–199.
Wernli H, Sprenger M. 2007. Identified and ERA-15 climatology of potential vorticity streamers and cutoffs near the extratropical tropopause. *J. Atmos. Sci.* **64**: 1569–1586.
Waugh DW, Funatsu BM. 2003. Intrusions into the tropical upper troposphere: Three dimensional structure and accompanying ozone and OLR distributions. *J. Atmos. Sci.* **60**: 637–653.
Waugh DW, Polvani LM. 2000. Intrusions into the tropical troposphere. *Geophys. Res. Lett.* **27**(23): 3857–3860.

